



The following Communications have been judged by at least two referees to be "very important papers" and will be published online at [www.angewandte.org](http://www.angewandte.org) soon:

D. S. Reddy, N. Shibata,\* J. Nagai, S. Nakamura, T. Toru,\*  
S. Kanemasa

**Desymmetrization-like Catalytic Enantioselective Fluorination of Malonates and Its Application to Pharmaceutically Attractive Molecules**

M. D. Pluth, R. G. Bergman,\* K. N. Raymond\*

**Catalytic Deprotection of Acetals in Basic Solution Using a Self-Assembled Supramolecular "Nanozyme"**

H. Herrmann, J. L. Fillol, H. Wadepohl, L. H. Gade\*

**Atom-by-Atom Assembly of  $EN_2^{2-}$  Units (E=S, Se) by Chalcogen Atom Transfer in the Coordination Sphere of a Transition Metal**

J.-E. Lee, J. Yun\*

**Catalytic Asymmetric Boration of Acyclic  $\alpha,\beta$ -Unsaturated Esters and Nitriles**

S.-T. Wu, Y.-R. Wu, Q.-Q. Kang, H. Zhang, L.-S. Long,\* Z. Zheng,\*  
R.-B. Huang, L.-S. Zheng

**Chiral Symmetry Breaking by Chemically Manipulating Statistical Fluctuation in Crystallization**

F. Arnesano, S. Scintilla, G. Natile\*

**Interaction between Platinum Complexes and a Methionine Motif Found in Copper Transport Proteins**

Self-Doped Conducting Polymers

Michael S. Freund, Bhavana Deore

Enzymatic Reaction Mechanisms

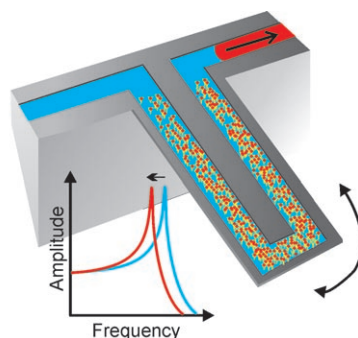
Perry A. Frey, Adrian D. Hegeman

## Books

reviewed by J. Heinze \_\_\_\_\_ 7922

reviewed by A. J. Kirby \_\_\_\_\_ 7922

**Weighing biomolecules:** Resonant cantilevers allow ultrasensitive weighing by detecting changes in the resonant frequency when mass is added to the cantilever. By placing the fluid inside the cantilever, particles can be measured sensitively under biologically relevant conditions and without labeling. Furthermore, cells can be weighed while flowing through the cantilever.

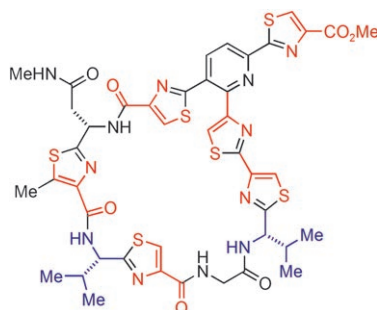


## Highlights

### Micro-electromechanical Systems

P. Tinnefeld\* \_\_\_\_\_ 7926 – 7929

Making Ultrasensitive Weighing Biocompatible by Placing the Sample within a Resonant Cantilever



**The building blocks of proteins**, the amino acids, also serve as precursors to a wide range of natural products. The thiopeptide antibiotics, molecules with remarkable molecular architectures, are wonderful examples of how nature elaborates simple  $\alpha$ -amino acids into complex arrays of heteroaromatic rings with potent biological activity. The picture shows the structure of amythiamicin D; its amino acid building blocks are highlighted in color.

## Reviews

### Thiopeptide Antibiotics

R. A. Hughes, C. J. Moody\* 7930 – 7954

From Amino Acids to Heteroaromatics—Thiopeptide Antibiotics, Nature's Heterocyclic Peptides

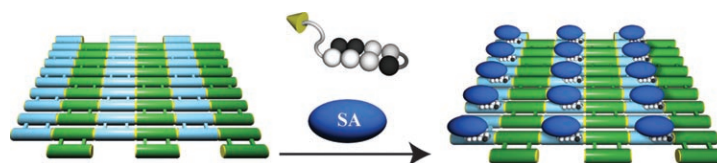
## Communications

### DNA Arrays

J. D. Cohen, J. P. Sadowski,  
P. B. Dervan\* ————— 7956 – 7959



Addressing Single Molecules on DNA Nanostructures



**Molecular glue:** A polyamide–biotin conjugate is capable of binding to specific sequences in a DNA nanostructure. These conjugates recruit streptavidin (SA) to a

two-dimensional array of DNA (see schematic representation) and do not require any prior modification of the DNA.

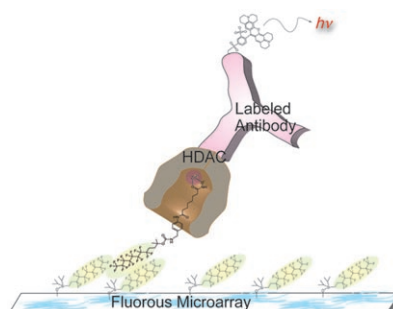


### Microarrays

A. J. Vegas, J. E. Bradner, W. Tang,  
O. M. McPherson, E. F. Greenberg,  
A. N. Koehler,  
S. L. Schreiber\* ————— 7960 – 7964



Fluorous-Based Small-Molecule Microarrays for the Discovery of Histone Deacetylase Inhibitors



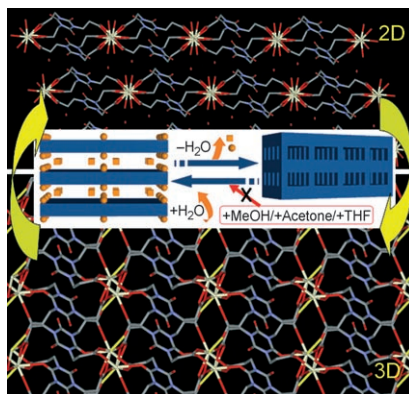
**Noncovalent immobilization** is an attractive method for identifying inhibitors of histone deacetylases (HDACs). Fluorous-based small-molecule microarrays were validated as an effective method. Three enzymes and three assays (microarray, biochemical activity, and surface plasmon resonance) were used to identify inhibitors of HDACs and to compare them.

### Framework Materials

S. K. Ghosh, J.-P. Zhang,  
S. Kitagawa\* ————— 7965 – 7968



Reversible Topochemical Transformation of a Soft Crystal of a Coordination Polymer



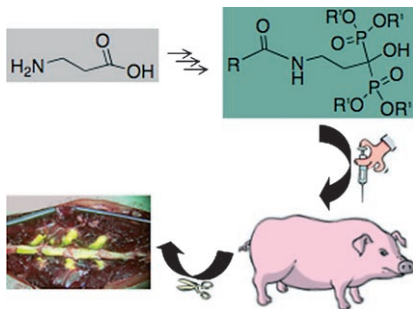
**Shaping up:** The two isomorphous 2D hybrid frameworks  $\{[Ln(tci)-(H_2O)_2] \cdot 2H_2O\}_n$  ( $Ln = Ce^{III}$  or  $Pr^{III}$ ,  $tciH_3 = \text{tris}(2\text{-carboxyethyl})\text{isocyanurate}$ ) were prepared using a highly flexible ligand. The frameworks show a single crystal to single crystal topochemical transformation from a two-dimensional (2D) to three-dimensional (3D) framework and vice versa (see picture) and exhibits selective adsorption properties of  $H_2O$  over MeOH and EtOH.

### For the USA and Canada:

ANGEWANDTE CHEMIE International Edition (ISSN 1433-7851) is published weekly by Wiley-VCH, PO Box 191161, 69451 Weinheim, Germany. Air freight and mailing in the USA by Publications Expediting Inc., 200

Meacham Ave., Elmont, NY 11003. Periodicals postage paid at Jamaica, NY 11431. US POSTMASTER: send address changes to *Angewandte Chemie*, Wiley-VCH, 111 River Street, Hoboken, NJ 07030. Annual subscription price for institutions: US\$ 7225/6568 (valid for print and

electronic / print or electronic delivery); for individuals who are personal members of a national chemical society prices are available on request. Postage and handling charges included. All prices are subject to local VAT/sales tax.



**No fly in this oinkment:** A targeted contrast agent allows real-time visualization of normal bones and hydroxyapatite crystals found in breast-cancer microcalcifications. Synthesis of the agent involves conjugation of a near-infrared fluorophore to methylester-protected pamidronate derivatives. Large-animal surgical models validate the effectiveness of the agent.

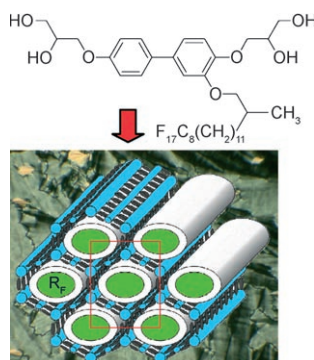
### Contrast Agents

K. R. Bhushan, E. Tanaka,  
J. V. Frangioni\* — 7969–7971

Synthesis of Conjugatable  
Bisphosphonates for Molecular Imaging  
of Large Animals



**To the bursting point:** The molecule shown forms a complex liquid-crystalline phase in which core-shell columns are embedded in a polygonal honeycomb formed by supramolecular cylinders (see picture;  $R_F$  = perfluorinated end groups). Temperature-induced anisotropic swelling of the cylinders occurs, and a transition to a lamellar phase is induced by “bursting” of the cylinders at the theoretical limit of the circumference-limited expansion.



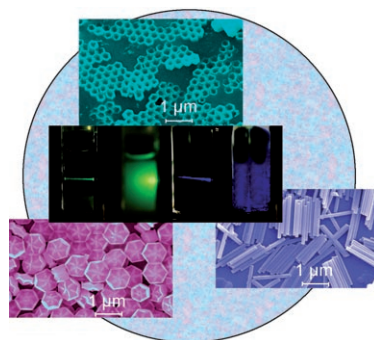
### Liquid Crystals

M. Prehm, F. Liu, U. Baumeister, X. Zeng,  
G. Ungar,\* C. Tschierske\* — 7972–7975

The Giant-Hexagon Cylinder Network—A  
Liquid-Crystalline Organization Formed  
by a T-Shaped Quaternary Amphiphile



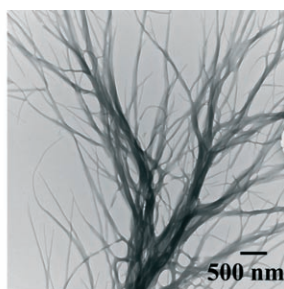
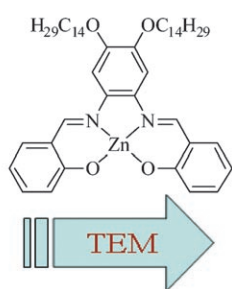
**Array of light:** Nanostructured arrays of  $\text{NaMF}_4$  ( $M$  = rare earth metal) can be prepared by a hydrothermal method. The arrays consist of nanoparticles with well-controlled morphologies (tubes, disks, or rods), phases (cubic or hexagonal), and sizes (80–900 nm). Multicolor upconversion fluorescence is realized in arrays of  $\text{NaYF}_4$  codoped with  $\text{Er}^{3+}$  and  $\text{Yb}^{3+}$  or with  $\text{Tm}^{3+}$  and  $\text{Yb}^{3+}$  (see picture).



### Hydrothermal Synthesis

F. Zhang, Y. Wan, T. Yu, F. Q. Zhang,  
Y. F. Shi, S. H. Xie, Y. G. Li, L. Xu, B. Tu,  
D. Y. Zhao\* — 7976–7979

Uniform Nanostructured Arrays of  
Sodium Rare-Earth Fluorides for Highly  
Efficient Multicolor Upconversion  
Luminescence



**Salphen the puzzle:**  $\text{Zn}(\text{salphen})$  complexes such as that shown organize into nanofibrils in the solid state. This assembly involves an intermolecular  $\text{Zn}\cdots\text{O}$  interaction that stabilizes a polymeric

structure with a  $(\text{ZnO})_n$  backbone. By tuning the peripheral substituents, luminescent gels may be prepared and the diameters of the fibers can be controlled.

### Nanofibers and Gels

J. K.-H. Hui, Z. Yu,  
M. J. MacLachlan\* — 7980–7983

Supramolecular Assembly of Zinc Salphen  
Complexes: Access to Metal-Containing  
Gels and Nanofibers



# Incredibly reader-friendly!



An aesthetically attractive cover picture that arouses curiosity, a well-presented and most informative graphical table of contents, and carefully selected articles that are professionally edited give *Angewandte Chemie* its distinctive character, which allows both easy browsing and further in-depth reading. Nearly 20 well-trained chemists, as well as eight further associates, work week in and week out to assemble reader-friendly issues and daily Early View articles online.

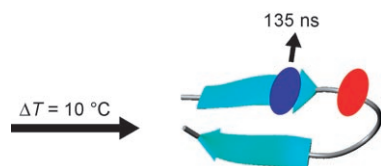


GESELLSCHAFT  
DEUTSCHER CHEMIKER



service@wiley-vch.de  
www.angewandte.org





**Fast dynamics and kinky turns:** The designed peptide PG12 forms a  $\beta$ -hairpin stabilized by a D-Pro enhanced type-II'  $\beta$  turn. Through a combination of  $^{13}\text{C}'$  isotope labels and temperature-jump nonlinear infrared spectroscopy local folding events were observed on a sub-microsecond timescale, in which the turn region remains structured during the temperature jump, and midstrand region opens up on a 130-ns timescale.

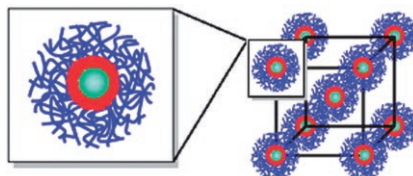
### Peptide Structural Dynamics

A. W. Smith, A. Tokmakoff\* **7984 – 7987**

Probing Local Structural Events in  $\beta$ -Hairpin Unfolding with Transient Nonlinear Infrared Spectroscopy



**ABC gel:** The triblock copolymer **PS-*b*-P2VP-*b*-PEO** undergoes simultaneous micellization and gelation, leading to high-storage-modulus materials that have fast responses to pH value, temperature, ionic strength, and shearing. The gel has a hierarchical structure (see picture) with spherical core-shell-corona micelles, which, in turn, pack closely into an ordered cubic structure.

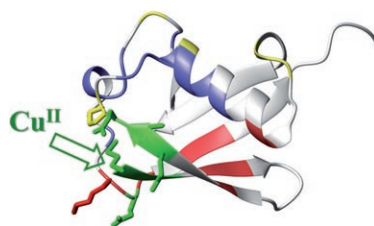


### Gels

N. Willet, J.-F. Gohy, L. Lei, M. Heinrich, L. Auvray, S. Varshney, R. Jérôme,\* B. Leyh **7988 – 7992**

Fast Multiresponsive Micellar Gels from Smart ABC Triblock Copolymer

**Appetite for copper:** Ubiquitin is a hallmark of toxic aggregates in neurodegenerative disorders, where metal ions are believed to play a crucial role. Copper(II) ions have been found to bind to ubiquitin at a specific site involving the N-terminal nitrogen of Met 1 and three oxygen donor ligands in a tetragonal geometry. The affinity of this site for copper(II) is comparable to that of other amyloidogenic proteins involved in neurodegenerative disorders.



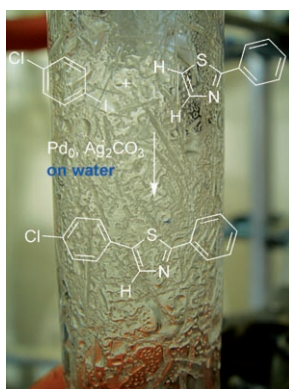
### Copper–Ubiquitin Binding

D. Milardi, F. Arnesano, G. Grasso, A. Magrì, G. Tabbì, S. Scintilla, G. Natile,\* E. Rizzarelli\* **7993 – 7995**

Ubiquitin Stability and the Lys 63-Linked Polyubiquitination Site Are Compromised on Copper Binding



**Wetter is better:** The direct arylation of thiazoles on water is quicker, cleaner, and higher-yielding than arylation in organic solvents. The reaction works under mild conditions for an array of aryl iodides, producing 2,5-diaryl thiazoles in excellent yields. Importantly, novel bi-heteroaryl compounds are produced without the requirement for stoichiometric organo-metallic coupling agents.



### Arylation of Heteroarenes

G. L. Turner, J. A. Morris, M. F. Greaney\* **7996 – 8000**

Direct Arylation of Thiazoles on Water



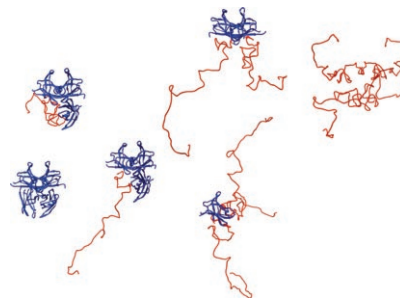
## Protein Structures

B. T. Ruotolo, S.-J. Hyung, P. M. Robinson,  
K. Giles, R. H. Bateman,  
C. V. Robinson\* ————— **8001–8004**



**Ion Mobility–Mass Spectrometry Reveals Long-Lived, Unfolded Intermediates in the Dissociation of Protein Complexes**

**Folded or not?** Ion mobility–mass spectrometry investigation of an activated macromolecular protein complex lends insight into the structures of intermediates formed in the dissociation process. The activated ions of human tetrameric transthyretin populate partially folded intermediate states (see picture; folded subunits in blue, partially unfolded subunits in red) prior to dissociation.

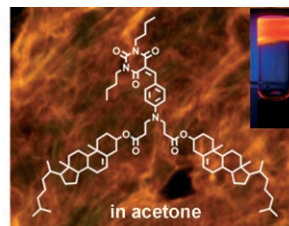
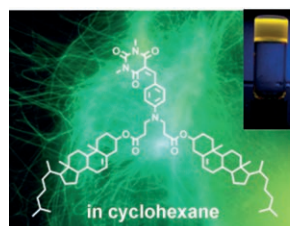


## Dye Assemblies

S. Yagai,\* M. Ishii, T. Karatsu,  
A. Kitamura ————— **8005–8009**



**Gelation-Assisted Control over Excitonic Interaction in Merocyanine Supramolecular Assemblies**



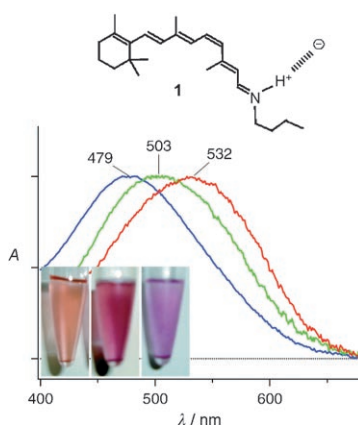
**Gelling together:** Merocyanine dyes possessing a cholesterol group as a gel-forming auxiliary self-assemble into nanoscopic fibers in apolar cyclohexane and polar acetone to form organogels, showing dramatically distinct optical

properties through exciton coupling. This dramatic change is a result of different chromophore packing arrangements within the nanoscopic fibers (see fluorescence microscopy images with photographs of the gels as insets).

## Color Tuning

Y. Furutani, K. Ido, M. Sasaki, M. Ogawa,  
H. Kandori\* ————— **8010–8012**

**Clay Mimics Color Tuning in Visual Pigments**



**Seeing is believing:** Protonated 11-*cis* retinal Schiff base RSB-11 (**1**), present in human blue and red pigments, varies in color when adsorbed onto the clay montmorillonite. The absorption spectra covers the entire visible range in clays from three different sources. Clays can thus mimic the carbon-based protein for color tuning of the chromophores in our vision.

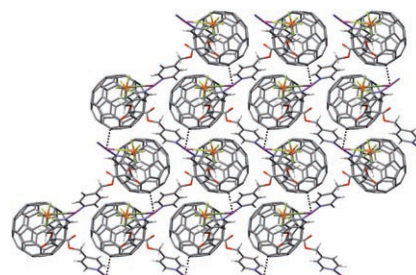
## Supramolecular Chemistry

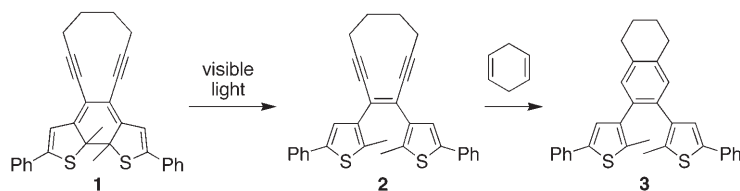
J. Fan, Y. Wang, A. J. Blake, C. Wilson,  
E. S. Davies, A. N. Khlobystov,\*  
M. Schröder\* ————— **8013–8016**



**Controlled Assembly of Silver(I)-Pyridylfullerene Networks**

**Stack them up!** Ag<sup>I</sup> ions combined with functionalized fullerenes (C<sub>60</sub>) form either discrete binuclear metallacycles or extended polymeric networks (see structure), depending on the geometry of the functional groups on the fullerene and conditions of assembly, such as choice of solvent.





**Visible changes:** Visible light is used to create an active enediyne for Bergman cyclization by taking advantage of a well-known molecular photoswitch. Only isomer **2** has the enediyne structure

required to produce a diradical that can be trapped as compound **3**. Isomer **2** is formed from the thermally stable isomer **1** by stimulating the ring-opening reaction with visible light.

### Photochemical Activation

D. Sud, T. J. Wigglesworth,  
N. R. Branda\* 8017–8019

Creating a Reactive Enediyne by Using Visible Light: Photocatalytic Control of the Bergman Cyclization

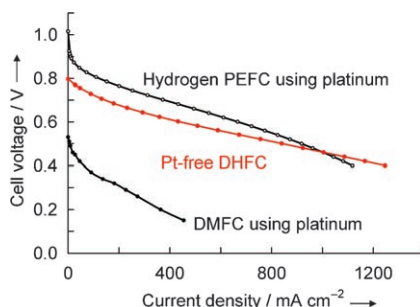


**Checking the traps:** When a phenyl selenide compound such as **1** was oxidized with sodium periodate or irradiated, an *ortho*-quinone methide intermediate formed and reacted with a DNA duplex by cross-linking. In the crystal structure of a derivative of **1** the biphenyl unit is twisted, and this might explain how **1** can interact effectively with the DNA backbone.

### DNA Cross-Linking

X.-C. Weng, L.-G. Ren, L.-W. Weng,  
J. Huang, S.-G. Zhu, X. Zhou,\*  
L.-H. Weng 8020–8023

Synthesis and Biological Studies of Inducible DNA Cross-Linking Agents

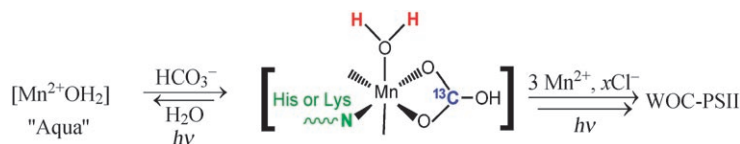


**Move over, platinum:** A Pt-free direct hydrazine fuel cell (DHFC), which uses an anion-exchange polymer electrolyte, shows a maximum power-generation performance of 0.5 W cm⁻² (1250 mA cm⁻² at 0.4 V). Its performance is comparable to that of the hydrogen polymer electrolyte fuel cell (PEFC) and far exceeds that of the direct methanol fuel cell (DMFC).

### Fuel Cells

K. Asazawa, K. Yamada, H. Tanaka,\*  
A. Oka, M. Taniguchi,  
T. Kobayashi 8024–8027

A Platinum-Free Zero-Carbon-Emission Easy Fuelling Direct Hydrazine Fuel Cell for Vehicles



**In the WOC:** The structural role of bicarbonate in the assembly of the Mn<sub>4</sub>Ca cluster of the water oxidizing complex (WOC) in photosystem II (PSII) is revealed by electron spin echo envelope modulation (ESEEM) spectroscopy. The

results clearly indicate the presence of C (from a labeled carbonate) and N (from histidine or lysine residue) in the inner coordination sphere of the Mn<sup>2+</sup> assembly intermediate.

### The Mn<sub>4</sub>Ca Cluster in PSII

J. Dasgupta, A. M. Tyryshkin,  
G. C. Dismukes\* 8028–8031

ESEEM Spectroscopy Reveals Carbonate and an N-Donor Protein-Ligand Binding to Mn<sup>2+</sup> in the Photoassembly Reaction of the Mn<sub>4</sub>Ca Cluster in Photosystem II

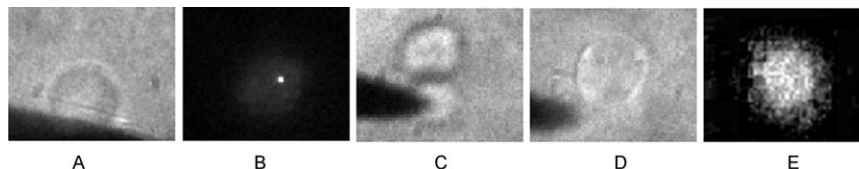


## Enzyme Catalysis

T.-M. Hsin, E. S. Yeung\* — 8032–8035



Single-Molecule Reactions in Liposomes



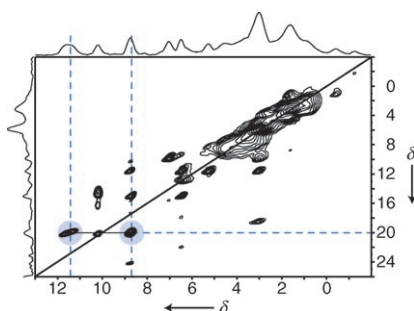
**Solitary confinement:** Single-molecule reactions were initiated by trapping and fusing liposomes and monitored by fluorescence imaging. The pictures show: an optical image of the liposome containing the enzyme (A), a fluorescence image of one labeled enzyme molecule in the

liposome (B), an optical image of the enzyme and substrate liposomes prior to electrofusion (C), an optical image of the fused liposome (D), and a fluorescence image of the fused liposome after incubation (E).

## Solid-State NMR Spectroscopy

J. M. Griffin, D. R. Martin,  
S. P. Brown\* — 8036–8038

Distinguishing Anhydrous and Hydrated Forms of an Active Pharmaceutical Ingredient in a Tablet Formulation Using Solid-State NMR Spectroscopy



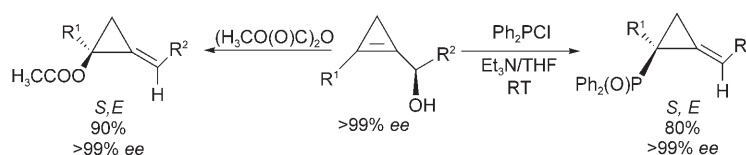
**With or without water?** In under two hours, an NMR spectroscopy experiment can determine whether the anhydrous form of an active pharmaceutical ingredient is present in a tablet formulation. Such a high-resolution spectrum constitutes a new analytical tool that should be routinely adopted in the characterization of pharmaceuticals.

## Synthetic Methods

A. Masarwa, A. Stanger,  
I. Marek\* — 8039–8042



An Efficient, Facile, and General Stereoselective Synthesis of Heterosubstituted Alkylidenecyclopropanes



**With just a nudge** (in the form of silica gel, an acidic ion-exchange resin, or heating at about 40 °C), the acetate derivatives of enantiomerically enriched cyclopropenyl alcohols undergo sigmatropic rearrangement to give alkylidenecyclopropanes with

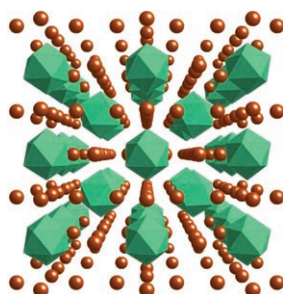
high *ee* values (see scheme). Similarly, the rearrangement of phosphinite derivatives at room temperature leads to phosphine oxide precursors of unusual chiral phosphine ligands.  $R^1$ ,  $R^2$  = alkyl, aryl.

## Actinide Chemistry

R. E. Wilson, S. Skanthakumar,  
P. C. Burns, L. Soderholm\* — 8043–8045

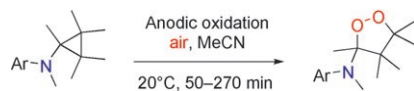


Structure of the Homoleptic Thorium(IV) Aqua Ion  $[\text{Th}(\text{H}_2\text{O})_{10}]\text{Br}_4$



**The homoleptic aqua complex of thorium(IV)** is the first aqua complex of a tetravalent cation to be isolated in the solid state. High-energy X-ray scattering experiments demonstrate the same ten-fold aqua coordination in solution. Green polyhedra  $[\text{Th}(\text{H}_2\text{O})_{10}]^{4+}$ , brown spheres  $\text{Br}^-$ .





**Electrical synthesizer:** Results of cyclic voltammetric studies on a range of aminocyclopropanes in the absence or in the presence of oxygen are in full agreement with the currently accepted autocatalytic mechanism for the aerobic oxidation of

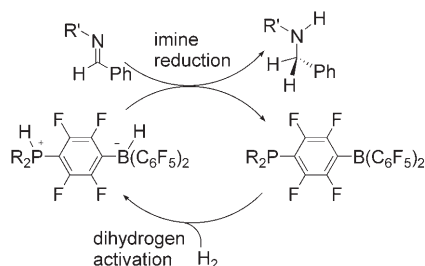
these compounds. A simple and efficient procedure was developed for the electro-synthesis of the corresponding endoperoxides (see scheme), some of which exhibit moderate antimalarial activity.

## Electrochemical Oxidation

C. Madelaine, Y. Six,\*

O. Buriez\* 8046–8049

Electrochemical Aerobic Oxidation of Aminocyclopropanes to Endoperoxides



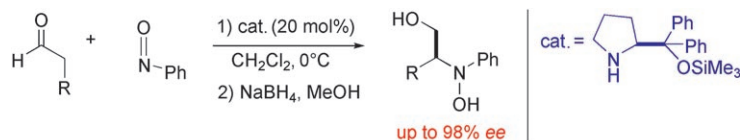
**Phosphonium borates** of the form  $R_2PH-(C_6F_4)BH(C_6F_5)_2$  are shown to be metal-free hydrogenation catalysts (see scheme) that effect reduction of sterically hindered imines and aziridines, as well as  $B(C_6F_5)_3$ -protected unhindered imines and nitriles, at relatively low  $H_2$  pressures and temperatures.

## $H_2$ Activation

P. A. Chase, G. C. Welch, T. Jurca,

D. W. Stephan\* 8050–8053

Metal-Free Catalytic Hydrogenation



**Donors not required:** External hydrogen-bond donors are not required for a highly regio- and enantioselective oxyamination reaction of aldehydes with nitrosobenzene (see scheme). The reaction proceeds in

the presence of the structurally simple organocatalyst (–)-(*S*)- $\alpha,\alpha$ -diphenylprolinol trimethylsilyl ether to afford the oxyaminated compounds in good yields.

## Organocatalysis

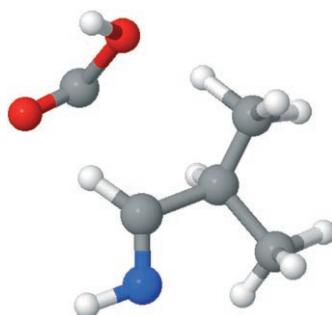
C. Palomo,\* S. Vera, I. Velilla, A. Mielgo,

E. Gómez-Bengoa 8054–8056

Regio- and Enantioselective Direct Oxyamination Reaction of Aldehydes Catalyzed by  $\alpha,\alpha$ -Diphenylprolinol Trimethylsilyl Ether



**Breaking up is hard to do:** The dominating negative-ion fragment formed by dissociative electron attachment (DEA) to amino acids or by their ionization through MALDI is  $[M-H]^-$ . Three different experimental techniques and molecular dynamics calculations are used to determine the site of hydrogen loss and which metastable decay pathways (for valine, see picture; blue nitrogen, red oxygen) dominate further decay.



## Ion Fragmentation

H. D. Flosadóttir, S. Denifl, F. Zappa,

N. Wendt, A. Mauracher, A. Bacher,

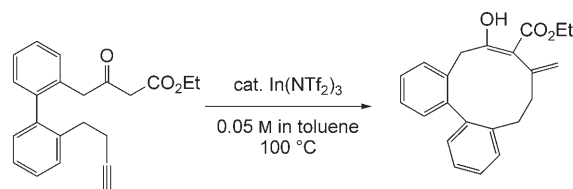
H. Jónsson, T. D. Märk, P. Scheier,

O. Ingólfsson\* 8057–8059

Combined Experimental and Theoretical Study on the Nature and the Metastable Decay Pathways of the Amino Acid Ion Fragment  $[M-H]^-$

## Medium-Sized Rings

H. Tsuji, K.-i. Yamagata, Y. Itoh,  
K. Endo, M. Nakamura,  
E. Nakamura\* — 8060 – 8062



Indium-Catalyzed Cycloisomerization  
of  $\omega$ -Alkynyl- $\beta$ -ketoesters into Six- to  
Fifteen-Membered Rings

**Many different sizes of rings available:**  
Heating  $\omega$ -alkynyl- $\beta$ -ketoesters in the presence of  $\text{In}(\text{NTf}_2)_3$  ( $\text{Tf}$  = trifluoromethanesulfonyl) produces six- to fifteen-membered ring products in good yields. The reaction features low catalyst loading and

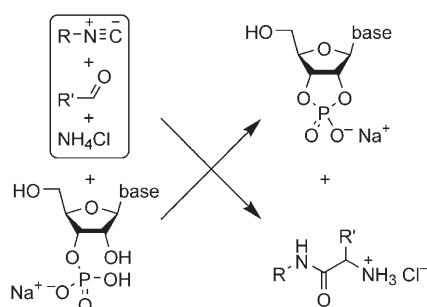
moderately dilute conditions, and the formation of medium-sized rings is sometimes faster than that for the corresponding six-membered rings. A synthesis of ( $\pm$ )-muscone is also reported.

## Multicomponent Reactions

L. B. Mullen,  
J. D. Sutherland\* — 8063 – 8066



Simultaneous Nucleotide Activation and  
Synthesis of Amino Acid Amides by a  
Potentially Prebiotic Multi-Component  
Reaction



**Prebiotic building blocks—two for the price of one:** In water at nearly neutral pH values, the assembly of an isocyanide, an aldehyde, and ammonia into an amino acid amide is facilitated by a nucleotide. In this process, the nucleotide is activated. The production of building blocks for both RNA and proteins in one high-yield reaction suggests a possible link between these macromolecules in the origin of life.

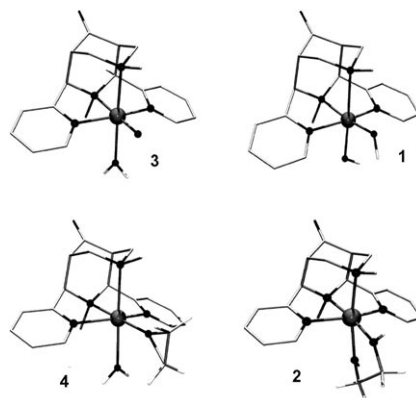
## Oxidation Catalysis

J. Bautz, P. Comba,\* C. Lopez de Laorden,  
M. Menzel, G. Rajaraman — 8067 – 8070



Biomimetic High-Valent Non-Heme Iron  
Oxidants for the *cis*-Dihydroxylation and  
Epoxidation of Olefins

**Pathfinding:** The iron(II) complex of the bispidine ligand  $\text{L}^1$  is oxidized with  $\text{H}_2\text{O}_2$  to intermediate-spin  $[(\text{L}^1)\text{Fe}^{\text{IV}}(\text{OH})_2]^{2+}$  (**1**, see picture) which forms *cis* diols **2** from olefins, and the high-spin  $[(\text{L}^1)\text{Fe}^{\text{IV}}=\text{O}(\text{OH}_2)]^{2+}$  ferryl complex (**3**) results in epoxidation (**4**). Product distributions (diol/epoxide) and  $^{18}\text{O}$  labeling studies are used to propose a mechanism, which is fully supported by DFT analyses.

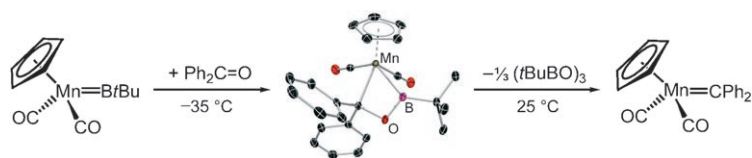


## Borylene Complexes

H. Braunschweig,\* M. Burzler, K. Radacki,  
F. Seeler — 8071 – 8073

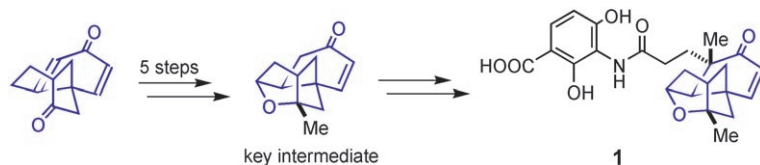


Borylene Metathesis through  
[2+2] Cycloaddition



**From Mn=B to Mn=C:** The first example of a concerted borylene metathesis through a clean cycloaddition–cycloreversion sequence is established, emphasizing the decisive influence of boron-bound

substituents, and alkyl groups in particular, on the reactivity of borylene complexes. Cyclic reaction intermediates were characterized by X-ray diffraction analysis.



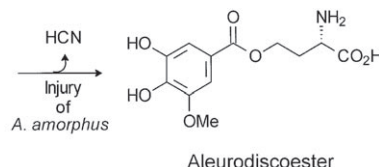
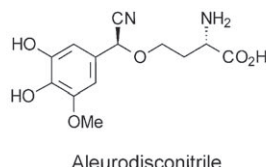
**Short cut:** In a new approach to the recently discovered antibiotic platensimycin (1), Nicolaou's late key intermediate is

synthesised without the use of protecting groups in five steps from a readily available starting material.

### Natural Product Synthesis

K. Tiefenbacher, J. Mulzer\* 8074–8075

Protecting-Group-Free Formal Synthesis of Platensimycin



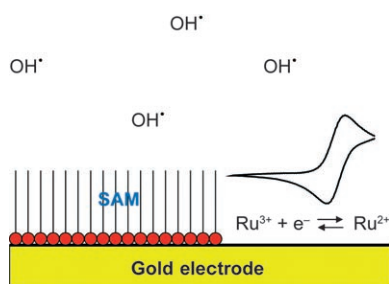
**A mighty midget!** When injured, the crust fungus *A. amorphus* (left in the picture) releases hydrocyanic acid by an oxidative mechanism so far unknown in nature. In contrast to cyanogenic glycosides in

which the smooth hydrolysis of the glycosidic bond is essential for the liberation of hydrocyanic acid, in aleurodisconitrile the oxidation-prone aromatic moiety enables the release of hydrocyanic acid.

### Chemical Defense

B. L. J. Kindler, P. Spiteller\* 8076–8078

Chemical Defense of the Crust Fungus *Aleurodiscus amorphus* by a Tailor-Made Cyanogenic Cyanohydrin Ether

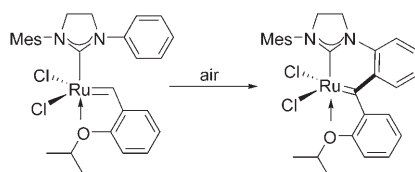


**Breaking cover:** Hydroxyl radicals  $\text{OH}^\bullet$  destroy the self-assembled monolayer (SAM) of hexanethiol on gold and mercury electrodes and thus allow the electrochemical response of the redox couple  $\text{Ru}^{2+/3+}$  to be measured. On a completely SAM-covered electrode the  $\text{Ru}^{2+/3+}$  signal is absent, thus the recovery of the signal following radical attack is a reliable measure of the radical activity.

### Analytical Methods

F. Scholz,\* G. López de Lara González, L. Machado de Carvalho, M. Hilgemann, K. Z. Brainina, H. Kahlert, R. S. Jack, D. T. Minh 8079–8081

Indirect Electrochemical Sensing of Radicals and Radical Scavengers in Biological Matrices



**Oxygen knocks it out:** Olefin metathesis catalysts without steric hindrance in the *ortho* positions of the *N*-aryl substituents can be transformed into catalytically inactive ruthenium complexes through C–H activation (see scheme). This process presumably proceeds by a pericyclic reaction and is rendered irreversible by oxygen.

### Ruthenium Alkylidene Complexes

K. Vehlouw, S. Gessler, S. Blechert\* 8082–8085

Deactivation of Ruthenium Olefin Metathesis Catalysts Through Intramolecular Carbene–Arene Bond Formation



Supporting information is available on the WWW (see article for access details).



A video clip is available as Supporting Information on the WWW (see article for access details).

## Sources

### Product and Company Directory

You can start the entry for your company in "Sources" in any issue of *Angewandte Chemie*.

If you would like more information, please do not hesitate to contact us.

Wiley-VCH Verlag – Advertising Department

Tel.: ☎ 62 01 - 60 65 65

Fax: ☎ 62 01 - 60 65 50

E-Mail: MSchulz@wiley-vch.de

## Service

Spotlights Angewandte's

Sister Journals \_\_\_\_\_ 7920 – 7921

Keywords \_\_\_\_\_ 8086

Authors \_\_\_\_\_ 8087

Preview \_\_\_\_\_ 8089



For more information on  
ChemMedChem see  
[www.chemmedchem.org](http://www.chemmedchem.org)